Thermochimica Acta 512 (2011) 110–117

Contents lists available at ScienceDirect

Thermochimica Acta

journal homepage: www.elsevier.com/locate/tca

Determination of standard enthalpy of vaporization and thermal decomposition reactions from derivative thermogravimetric (DTG) curves

S. Kolay[a], R. Mishra[a], D. Das[a], S.R. Dharwadkar[b,*]

[a] Chemistry Division, Bhabha Atomic Research Centre Trombay, Mumbai 400 085, India
[b] Department of Chemistry, Mumbai University, Kalina Campus, Mumbai, Maharashtra 400 098, India

ARTICLE INFO

Article history:
Received 29 January 2010
Received in revised form 1 July 2010
Accepted 9 September 2010
Available online 25 September 2010

Key words:
Vapor pressure
Dissociation pressure
Enthalpy of vaporization
Enthalpy of decomposition
Derivative thermogravimetry

ABSTRACT

The paper proposes the use of the derivative thermogravimetric (DTG) curve for the acquisition of equilibrium vapor pressure and dissociation pressure for the materials and derivation of their standard enthalpy of formation from single DTG curve recorded under optimum experimental conditions, such as heating rate and the sweep rate of the carrier gas passed over the sample. The vapor pressure and the standard enthalpy of sublimation ($\Delta_{sub}H^{\circ}_{298.15}$) of CdI_2 and the dissociation pressure and the standard enthalpy of formation of $CaCO_3$ derived from their DTG curves are found to be in good agreement with the best assessed values reported in the literature.

1. Introduction

Vapor pressure measurements have been frequently used in the determination of thermodynamic data for the condensed phases [1–7]. Among the several techniques available for vapor pressure measurements [8–10] the transpiration, which is also known as the gas entrainment technique is more versatile and enables determination of the vapor pressure of the materials over a wide range of pressures in the presence of large amount of the desired reactive as well as inert ambient gaseous atmosphere [2,9,13]. This technique, proposed originally by Regnault for the determination of the vapor pressure of liquids [11] has undergone several innovations and improvements and has been utilized in recent years for the acquisition of the vapor pressure and other thermodynamic stability data over a wide temperature range, for the most complex systems including high temperature ceramics, metals and alloys [2,3,6,7].

1.1. The principle of transpiration technique

The transpiration technique essentially involves measurement of the number of moles of the vapor of the condensed phase transported by the known volume of the carrier gas swept over the sample located in uniform temperature zone of the furnace, without disturbing the thermodynamic equilibrium between the vapor and the condensed phase undergoing vaporization at the desired temperature. The experiments involve two steps:

1. determination of apparent vapor pressure at different flow rates at the selected temperature to identify the range of flow rates over which the vapor pressure is independent of the flow rates employed, a criterion which ensures that the condensed phase is virtually in equilibrium with its vapor and
2. measurement of the vapor pressure of the materials at different temperatures at "the selected flow rate" chosen from the flow rate independent region.

The enthalpy of vaporization and other thermodynamic quantities are then derived from the vapor pressure data employing the Gibbs Helmholtz equation [12].

1.2. Measurement of vapor pressure by transpiration technique

In a typical transpiration experiment, the material for which the vapor pressure has to be measured is contained in a boat located in the uniform temperature zone of the tubular horizontal or vertical furnace. The vapor generated above the sample is swept away by the carrier gas, condensed in the colder region downstream and analyzed. Alternately, in few cases, where the sample under investigation is non-hygroscopic and the sample container does not undergo any significant mass change during heating, the mass loss of the sample due to vaporization is determined by weighing

* Corresponding author. Tel.: +91 22 26153470.
E-mail address: srdhawadkar@hotmail.com (S.R. Dharwadkar).

0040-6031/$ – see front matter © 2010 Elsevier B.V. All rights reserved.
doi:10.1016/j.tca.2010.09.010

the sample before and after the experiment. The vapor pressure is then calculated, knowing the amount of the vapor swept by the unit volume of the carrier gas and the molecular weight of the vapor species. The molecular weight of the vapor species has to be known or determined prior to the detailed vapor pressure measurements. Merten and Bell [13] and more recently Kvande and Wahlbeck [14] have presented excellent reviews of this technique.

In conventional transpiration method, the experiment performed at each flow rate and temperature has to be terminated in order to determine the number of moles of the vapor of the sample under investigation transported by the known volume of the carrier gas. The condenser has to be taken out of the assembly, for the chemical analysis of the vapor deposited in it or the boat containing the sample should be taken out and weighed to assess the mass loss during the vaporization process. This process, besides being tedious and time consuming is prone to large experimental errors.

1.3. Automatic recording transpiration system for vapor pressure measurement

Dharwadkar and his co-investigators [15] designed and fabricated an automatic recording assembly to measure the vapor pressure by transpiration technique. The assembly was built incorporating the electronic microbalance used for continuous monitoring of the mass loss of the sample during vaporization. All the measurements at different flow rates and temperatures could be done on a single sample by automatic recording of the mass loss of the sample during vaporization, without interrupting the experiment or dismantling the experimental assembly, thereby reducing the experimental time to a very large extent.

2. The objective of the present investigation

In the present paper we attempted the use of a single derivative thermogravimetric (DTG) curve recorded for the congruent vaporization of CdI_2 for acquisition of its vapor pressure and determination of the standard enthalpy of vaporization. Similar procedure was employed to obtain the dissociation pressure and standard enthalpy of decomposition of $CaCO_3$. The standard enthalpy of formation of these compounds could also be derived from these data. This approach reduced the time duration of the experiment still further, since it involved the use of a single DTG curve recorded at the slowest heating rate, unlike in the conventional method in which several isothermal experiments have to be performed at different temperatures for acquisition of vapor pressure/dissociation pressure data in order to evaluate the standard enthalpy change for the process under consideration.

2.1. The methodology for acquisition of thermodynamic data from the DTG curve

It can be shown that the ordinate of the DTG curve at any temperature represents the measure of the vapor pressure/dissociation pressure of the material at that temperature, if the equilibrium exists between the condensed phase and the vapor. The DTG curve recorded at the slowest heating rate and moderate flow rate of the carrier gas is expected to facilitate the attainment of instantaneous equilibrium between the condensed phase and the vapor at each temperature if the kinetic barrier for the vaporization/dissociation process is minimal or virtually absent. The instantaneous rate of mass loss at any temperature derived from the ordinate of the DTG curve could under these conditions represents the isothermal rate of mass loss at that temperature.

2.2. The relation between the vapor pressure and the ordinate (dm/dT) of the DTG curve

The vapor pressure P_v in transpiration experiment at any chosen temperature can be expressed as

$$P_v = \frac{n_v}{(n_c + n_v)} P \tag{1}$$

where n_v represents the number of moles of the vapor transported by n_c number of moles of the carrier gas from the vaporizing system and P is the total pressure in the reaction chamber, generally maintained at 1 atm. The number of moles of vapor 'n_v' is obtained from the mass loss of the material, where as the number of moles of the carrier gas 'n_c' is calculated from the volume of the carrier gas swept over the sample. The use of Eq. (1) implies that the mixture of the vapor and carrier gas behaves ideally and the vapor is transported mainly by the carrier gas. The relative contribution by diffusion to the total vapor transport is assumed to be negligible. Eq. (1) can be rewritten by dividing the numerator and the denominator by time 't' as

$$P_v = \frac{n_v/t}{(n_c/t + n_v/t)} P \tag{2}$$

Generally, n_v is very small compared to n_c, hence Eq. (2) can be expressed as

$$P_v = \frac{dn_v/dt}{dn_c/dt} P \tag{3}$$

The numerator dn_v/dt in Eq. (3) can be expressed as

$$\frac{dn_v}{dT} \times \frac{dT}{dt} = \frac{dn_v}{dT} \times \beta \tag{4}$$

where β is the heating rate and dn_v/dT represents the term proportional to the ordinate dm/dT of the DTG curve. Eq. (3) can now be rewritten as

$$P_v = \frac{(dn_v/dT) \times \beta}{dn_c/dt} P \tag{5}$$

Eq. (5) can now be applied to the derivative thermogravimetric curve and the vapor pressure can be expressed in terms of the ordinate of the DTG curve. The term dn_v/dT on the right hand side of Eq. (5) represents the ordinate of the DTG curve and β is the heating rate. The term dn_c/dt in the denominator in Eq. (5) represents the rate of flow of carrier gas swept over the sample. Thus, in principle it is possible to derive the vapor pressure and determine the corresponding thermodynamic parameters for the materials at any temperature using the DTG data recorded under near equilibrium condition.

In the present paper the equilibrium vapor pressure of CdI_2 and dissociation pressure of $CaCO_3$ have been determined using DTG data obtained under near equilibrium condition employing a commercial thermogravimetric apparatus. The thermodynamic data derived for CdI_2 using the DTG curve were compared with the vapor pressure and enthalpy of vaporization values reported previously from this laboratory obtained using automatically recording conventional transpiration setup [15] and other data derived from high temperature mass spectrometric vapor pressure measurements [16]. The values of vapor pressure and enthalpy of vaporization of CdI_2 derived from the DTG curve are found to be in good agreement obtained previously by conventional transpiration technique [15]. The enthalpy of vaporization value derived from the vapor pressure values obtained from the mass spectrometric vapor pressure measurements [16] by extrapolation to the temperature range of the present investigation, employing the third law treatment was in close agreement with that derived from the present work. The absolute pressure values at each temperature however, differed from

the values obtained in the present studies by a constant factor of about two.

Similar studies carried out for the thermal decomposition of $CaCO_3$ with a view to check the validity of using this approach for the heterogeneous incongruent decomposition reactions showed good agreement of the dissociation pressure of $CaCO_3$ and the standard enthalpy of its dissociation with the values previously reported in standard thermodynamic compilation [17] and the simultaneously reported results obtained by conventional transpiration technique [18].

The results on $CaCO_3$ obtained in this work employing the DTG were corroborated by recording the inception temperatures of DTG at different partial pressures of CO_2 and deriving the enthalpy of the decomposition reaction from the shift observed in this temperature with the increasing partial pressure of CO_2 in Ar–CO_2 mixture.

3. Experimental

3.1. Thermogravimetric system and mass measurements

The thermogravimetric curves for pure CdI_2 (BDH, AnalaR Grade, >99%) and $CaCO_3$ (GR, Merk, >99.5%) samples were recorded in flowing argon and Ar–CO_2 mixtures at the flow rates ranging between 0.2 and 16 ml/min, employing a simultaneous recording bottom loading TG–DTA system supplied by SETARAM, France (Model SETSYS), having room temperature sensitivity of 1 μg, at the heating rates of 5 and 1 K/min. The mass measurements in the bottom loading thermogravimetric systems of the type used in the present studies are prone to significant errors caused due to apparent mass changes resulting from buoyancy and thermo molecular forces (in case the instrument is operated in vacuum), particularly when such thermo balances are employed at high sensitivities. The simultaneously recording TG/DTA instrument used in the present work has the provision to correct such errors by first recording the TG run without the sample in the pan (blank run), prior to the experiment carried out with the sample. The "blank runs" were therefore recorded with empty sample pan under similar experimental conditions of constant heating rates and carrier gas flow rate, prior to the experiments carried out with the sample and the data were used to obtain the corrected TG curve.

3.2. Measurement of the gas flow rate

The different flow rates (0.2–16 ml/min) used in the experiments for establishing the equilibrium vaporization condition were obtained using the mass flow controller provided with the thermogravimetric system. The correct functioning of the mass flow meter was verified using the soap bubble technique. The flow rate of the carrier gas in any given experiment could be reproduced within 1%.

3.3. Temperature calibration of the TG system

The temperature calibration of the instrument was done employing the polymorphic phase transformations in KNO_3, quartz and $BaCO_3$ [19]. The accuracy in the measured temperature was found to be within ±1 K and the temperature control was better than ±0.5 K at the set temperature.

3.4. Mass calibration

The mass calibration of the thermobalance was done by following thermal decomposition of $CaC_2O_4{\cdot}H_2O$. The mass loss steps involved in the thermal decomposition of anhydrous oxalate to carbonate and the subsequent decomposition of $CaCO_3$ to CaO were used for mass calibration. The DTG curves were obtained from the

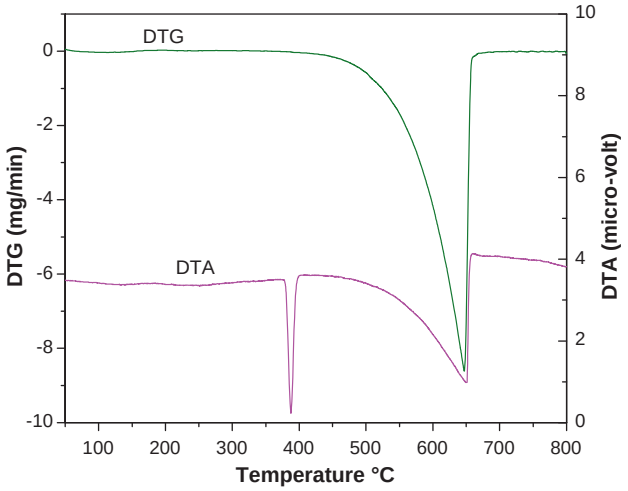

Fig. 1. Simultaneously recorded DTG and DTA curves for the vaporization of CdI_2 in flowing Ar (8 ml/min) at 5 K/min.

TG curves corrected for the apparent mass change, using the available software. The amount of sample used in each experiment was limited by the capacity of the sample holder and the total percentage of the mass change involved in the reaction. The CdI_2 samples weighing in the range 30–50 mg were taken in the platinum cups with the total exposed surface area of nearly 60 mm × 60 mm. The amount of $CaCO_3$ used in each experiment ranged between 10 and 15 mg.

3.5. Recording of the DTG curves

The DTG curves for the vaporization of CdI_2 were recorded in pure flowing argon. The similar curves for thermal decomposition of $CaCO_3$ were however recorded in pure argon and argon–carbon dioxide mixtures in the range 25–75% of CO_2 in order to study the influence of the ambient CO_2 pressure on the decomposition temperature of $CaCO_3$. The flow rate of the Ar–CO_2 mixture in these measurements was maintained at 8 ml/min. All the DTG curves used in the acquisition of thermodynamic data were recorded at the constant heating rate of 1 K/min.

4. Results

4.1. Vaporization of cadmium iodide

Fig. 1 represents the typical simultaneously recorded DTG and DTA curves for the vaporization of CdI_2 sample recorded in argon flowing at the rate of 8 ml/min, employing the heating rate of 5 K/min. The DTA curve indicates melting of CdI_2 prior to vaporization. A typical DTG curve derived from the thermogravimetric (TG) curve recorded for molten CdI_2 at 1 K/min in flowing argon (flow rate 8 ml/min) is presented in Fig. 2. Derivation of vapor pressure from this curve needs prior knowledge of the thermodynamic equilibrium existing between the condensed phase (CdI_2) and its vapor. The region of flow rate in which the equilibrium exists between CdI_2 liquid and its vapor has to be concluded from the plot of the apparent pressure versus the flow rate. The region in which the apparent pressure is independent of the flow rate is indicative of the thermodynamic equilibrium between the CdI_2 liquid and its vapor. Fig. 3 shows the plot of apparent pressure of CdI_2 calculated using Eq. (2) (imposing the condition that $n_c \gg n_v$) versus the flow rate obtained from the isothermal vaporization measurements at 757 K, the mean temperature of the measurements selected from the DTG curve. The values of these pressures at different flow rates are listed

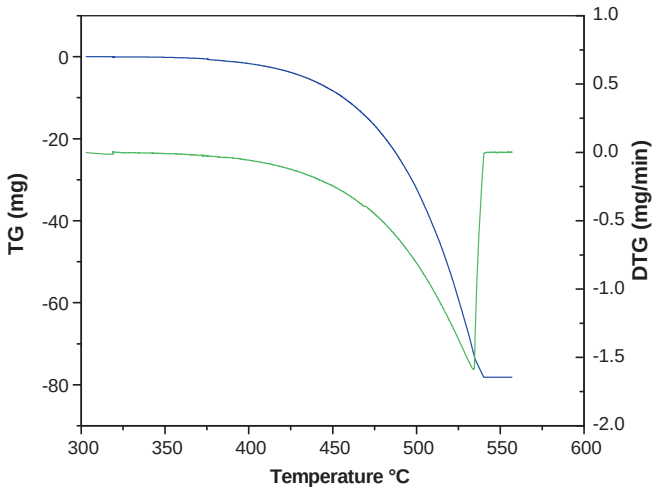

Fig. 2. Simultaneous TG and DTG plot for CdI_2 in flowing Ar (8 ml/min) at the heating rate of 1 K/min.

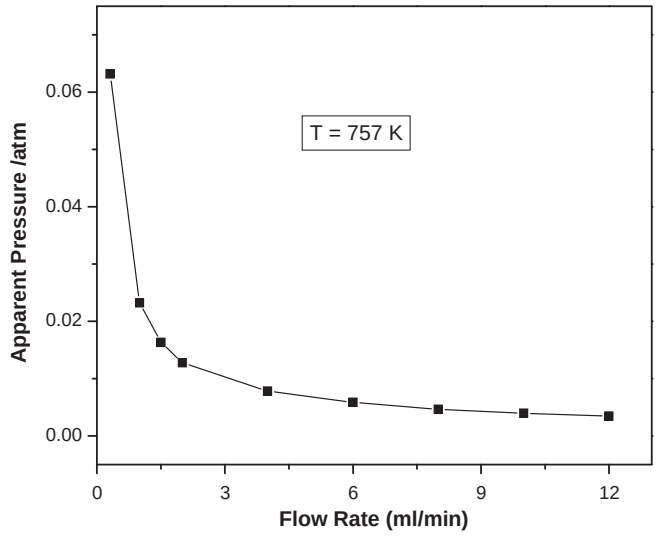

Fig. 3. The plot of apparent vapor pressure (atm) of CdI_2 (l) as a function of flow rate of Ar (ml/min) at 757 K.

in Table 1. The plot of apparent pressure versus the flow rate (Fig. 3) yielded the plateau in flow range between 4 ml/min and 12 ml/min, indicating that the carrier gas is saturated with the CdI_2 vapor and thermodynamic equilibrium exists between the condensed phase and the vapor in the region of this flow rate. The vapor pressure values at different temperatures derived from the ordinates of the DTG curve recorded at the heating rate of 1 K/min and 1 atm mean pressure of the argon gas flowing over the sample at the rate of 8 ml/min, using Eq. (5) are listed in Table 2. The plot of $\ln p(CdI_2(atm))$ versus

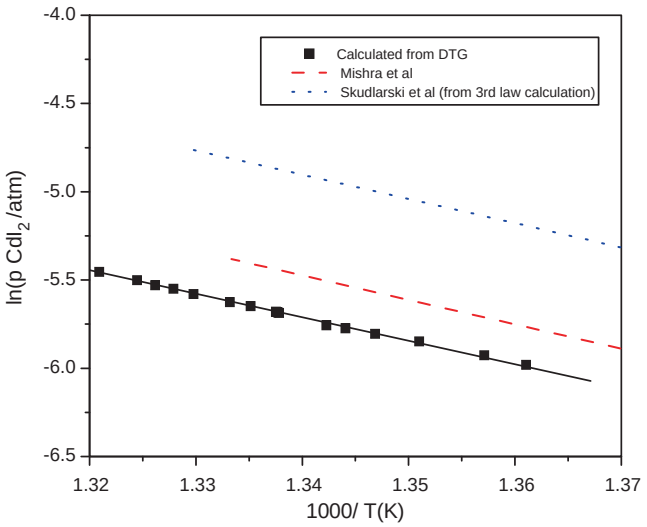

Fig. 4. The plot of $\ln p(CdI_2(l)(atm))$ as a function of $1/T$ (K).

$1/T$ (Fig. 4) yielded the straight line which could be expressed by Eq. (6).

$$\ln\ p(CdI_2(atm))(\pm 0.007) = \frac{-13335.7(\pm 85.6)}{T} + 12.16(\pm 0.12) \quad (6)$$

The value of enthalpy of vaporization derived from the slope of this plot at the mean temperature of the experiment was found to be 110.9 kJ/mol and compared very well with the value 115.2 kJ/mol derived from the conventional transpiration measurements reported earlier from this laboratory [1]. The $\ln p(CdI_2(atm))$ versus $1/T$ relation for these measurements could be expressed by Eq. (7)

$$\ln\ p(CdI_2(atm))(\pm 0.007) = \frac{-13856.4(\pm 21.4)}{T} + 13.09(\pm 0.029) \quad (7)$$

The standard enthalpy of sublimation of CdI_2 at 298.15 K derived from the DTG curve employing the heat capacity values in Ref. [17] is found to be 144.2 ± 2.1 kJ/mol compared to 148.5 ± 7.6 kJ/mol reported earlier from this laboratory [1] from conventional transpiration experiments and 146.8 ± 0.2 kJ/mol reported by Skudlarski et al. [16] derived by third law treatment of the vapor pressure values of solid CdI_2 measured by Knudsen effusion mass spectrometry. The vapor pressure values calculated from the DTG curve and those derived from our earlier reported [1] isothermal transpiration measurements (by extrapolation from 715 K) at some selected temperatures are compared in Table 2. The values of vapor pressure of liquid CdI_2 in the temperature range of the present investigation were derived from Knudsen effusion mass spectrometric vapor pressure measurements by Skudlarski et al. [16] on solid CdI_2, by the third law method, using their standard enthalpy of sublimation CdI_2 (146.8 kJ/mol) at 298.15 K and the difference in free energy functions for liquid and vapor CdI_2 taken from Ref. [17]. These val-

Table 1
The values of the apparent vapor pressures of CdI_2 (l) at 757 K for different flow rates.

Flow rate (ml/min)	No. of carrier gas molecules (n_c/s)	DTG (mg/min)	No of vapor molecules (n_v/s)	$P_{apparant} = (n_v/n_c) \times P^\circ$ (where $P^\circ = 1$ atm)
12.00	5.377×10^{18}	0.675	1.850×10^{16}	3.44×10^{-3}
10.00	4.481×10^{18}	0.650	1.782×10^{16}	3.98×10^{-3}
8.00	3.585×10^{18}	0.604	1.656×10^{16}	4.62×10^{-3}
6.00	2.690×10^{18}	0.576	1.579×10^{16}	5.87×10^{-3}
4.00	1.792×10^{18}	0.512	1.403×10^{16}	7.83×10^{-3}
2.00	0.896×10^{18}	0.417	1.143×10^{16}	1.28×10^{-2}
1.50	0.672×10^{18}	0.400	1.096×10^{16}	1.63×10^{-2}
1.00	0.448×10^{18}	0.380	1.042×10^{16}	2.32×10^{-2}
0.31	0.139×10^{18}	0.320	0.877×10^{16}	6.32×10^{-2}

Table 2
Comparison of the vapor pressure data of CdI_2 (l) derived from DTG measurements at the flow rate of 8 ml/min and the literature values in the selected temperature range.

Temperature (K)	Vapor pressure of CdI_2 (l) derived from DTG (atm)	Vapor pressure of CdI_2 (l) derived from Eq. (7) (atm)	Vapor pressure of CdI_2 (l) derived from Eq. (8) (atm)
740	2.85×10^{-3}	3.57×10^{-3}	6.37×10^{-3}
745	3.21×10^{-3}	4.05×10^{-3}	7.22×10^{-3}
750	3.62×10^{-3}	4.58×10^{-3}	8.16×10^{-3}
755	4.07×10^{-3}	5.18×10^{-3}	9.22×10^{-3}
760	4.57×10^{-3}	5.84×10^{-3}	1.04×10^{-2}
765	5.13×10^{-3}	6.58×10^{-3}	1.17×10^{-2}
770	5.75×10^{-3}	7.41×10^{-3}	1.31×10^{-2}

ues are also listed in Table 2 and plotted in Fig. 4. Eq. (8) gives the vapor pressure of CdI_2 (l) derived from the data reported by Skudlarski et al. [16] in the liquid range of the present DTG investigation

$$\ln\ p(CdI_2(atm)) = \frac{-13753.43(\pm 18)}{T} + 13.53(\pm 0.024) \quad (8)$$

It can be concluded from Fig. 4 that there is a good agreement in the absolute pressures as well as the enthalpy of the vaporization of liquid CdI_2 derived from a single DTG experiment in the present work and that obtained by conventional isothermal transpiration experiments [1]. The observed difference in the vapor pressure of CdI_2 could result due to difference in purity of the sample employed in the two experiments. However, the purity of CdI_2 used in the present experiments and in the work reported in Ref. [1] is same since the material was obtained from the same vendor (BDH, AnalaR) and hence this difference could not be accounted for on the basis of the difference in purity of the sample. The observed difference of about 20% in the vapor pressure between these two methods is however acceptable in the high temperature chemistry measurements. Though there is a good agreement in the enthalpy values obtained in these two methods and that derived from Knudsen effusion mass spectrometric measurements [16], the absolute pressure calculated from Eq. (8) is higher nearly by a factor of two, indicating some systematic error in the mass spectrometric measurement. The difference in the vapor pressure values derived by extrapolation of the data by Skudlarski et al. in the present temperature range (Fig. 4) involves a phase transformation and large temperature extrapolation. This could be one of the sources of errors. Besides, the error in the vapor pressure derived from the mass spectrometric data can also arise due to conversion factors employed to convert ion intensity to pressure, which includes several terms such as ionization cross section of the vapor, electron multiplier efficiency, Clausing factor for the Knudsen orifice etc. [16]. The extent to which these factors would contribute to the total error is however, uncertain.

4.2. Thermal decomposition of calcium carbonate

The DTG curve for thermal decomposition of $CaCO_3$ recorded at the heating rate of 1 K/min in argon at the flow rate of 4 ml/min is shown in Fig. 5. Similar curve was also recorded at the flow rate of 2 ml/min. The plot of apparent pressure of CO_2 versus the flow rate at 993 K indicated the rapid decrease of the pressure with the increasing flow rate between 0.2 and 2 ml/min. The pressure remained virtually constant between 2 and 4 ml/min. The values of apparent pressures at different flow rates at 993 K are listed in Table 3 and are plotted in Fig. 6. The dissociation pressure values of $CaCO_3$ derived from the ordinates of the DTG curve at some selected temperatures are listed in Table 4. The plot of ln of dissociation pressure of CO_2 calculated from the ordinates of the DTG curves (recorded at 2 and 4 ml/min) versus the reciprocal of absolute temperature yielded the straight lines shown in Fig. 7. The equations for linear least square fit for the $\ln p(CO_2)$ versus $1/T$ plots obtained from the DTG curves recorded at the flow rates of 2 and 4 ml/min

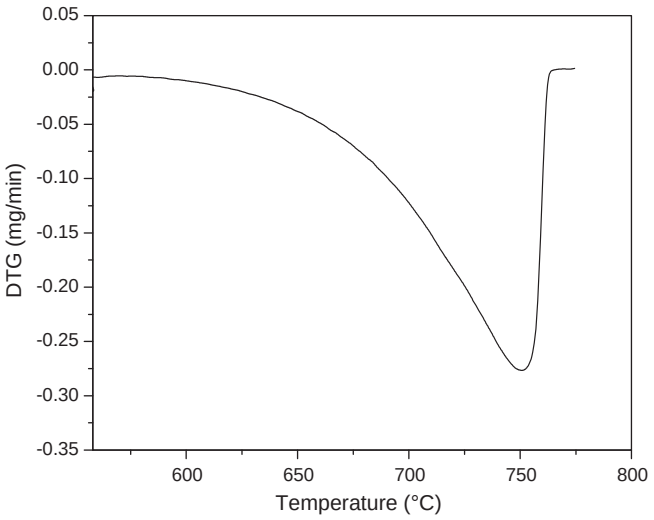

Fig. 5. DTG plot for $CaCO_3$ in flowing argon (4 ml/min) at the heating rate of 1 K/min.

could be expressed by Eqs. (9) and (10), respectively which can be written as

$$\ln\ p(CO_2(atm)) = \frac{-20795.2 \pm 56.41}{T} + 17.78 \pm 0.06 \quad (9)$$

$$\ln\ p(CO_2(atm)) = \frac{-20791.6 \pm 51.29}{T} + 17.20 \pm 0.05 \quad (10)$$

The dissociation pressure values in Eqs. (9) and (10) were derived ignoring the term n_v in the denominator in Eq. (1). The pressures calculated including the term n_v in the denominator of this equation are also listed in Table 4. The linear least squares fit for the data corrected for n_v could be expressed by Eqs. (9a) and

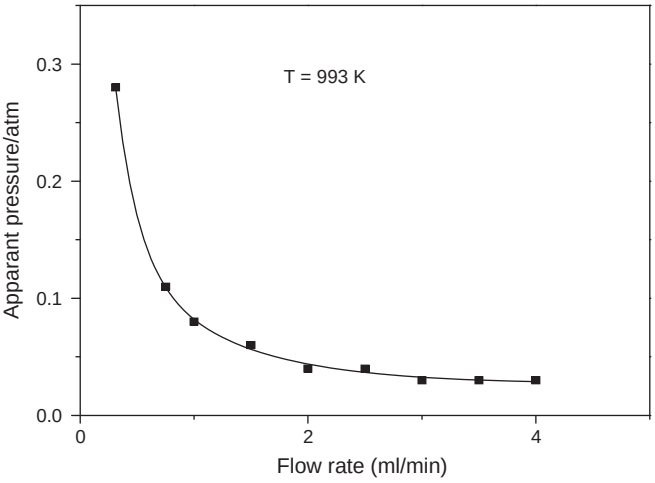

Fig. 6. Plot of apparent dissociation pressure (atm) of $CaCO_3$ as a function of flow rate of Ar (ml/min) at 993 K.

Table 3
The values of the apparent dissociation pressures of $CaCO_3$ at 993 K for different flow rates.

Flow rate (ml/min)	DTG (mg/min)	No. of carrier gas molecules (n_c/s)	No of vapor molecules (n_v/s)	$P_{apparant} = (n_v/n_c) \times P^\circ$ (where $P^\circ = 1$ atm)
0.31	0.173	1.389×10^{17}	3.947×10^{16}	0.28
0.75	0.169	3.361×10^{17}	3.855×10^{16}	0.12
1.00	0.166	4.481×10^{17}	3.787×10^{16}	0.08
1.50	0.167	6.722×10^{17}	3.810×10^{16}	0.06
2.00	0.178	8.963×10^{17}	4.061×10^{16}	0.04
2.50	0.191	1.120×10^{18}	4.357×10^{16}	0.04
3.00	0.200	1.344×10^{18}	4.563×10^{16}	0.03
3.50	0.205	1.568×10^{18}	4.677×10^{16}	0.03
4.00	0.204	1.792×10^{18}	4.654×10^{16}	0.03

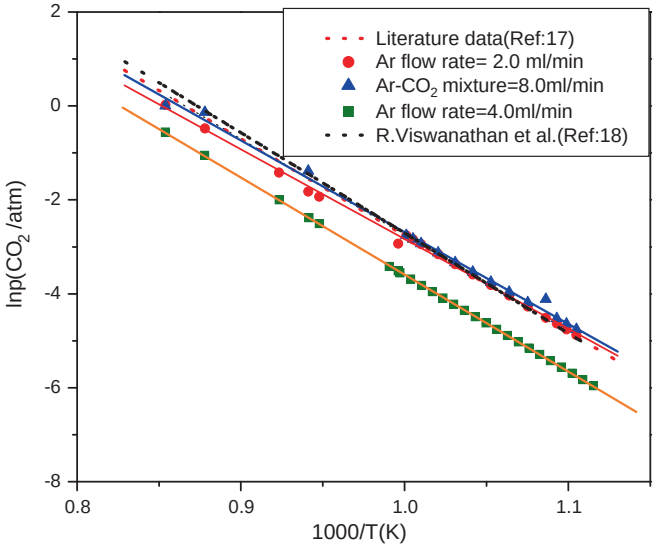

Fig. 7. The plot $\ln p(CO_2(atm))$ as function of $1/T$ (K).

(10a), respectively.

$$\ln\ p(CO_2(atm)) = \frac{-20407.6 \pm 29.78}{T} + 17.35 \pm 0.03 \qquad (9a)$$

$$\ln\ p(CO_2(atm)) = \frac{-20574.74 \pm 18.43}{T} + 16.96 \pm 0.02 \qquad (10a)$$

A typical plot for indicating the influence of ignoring n_v term in Eq. (1) on $\ln p$ versus $1/T$ plot is shown in Fig. 8.

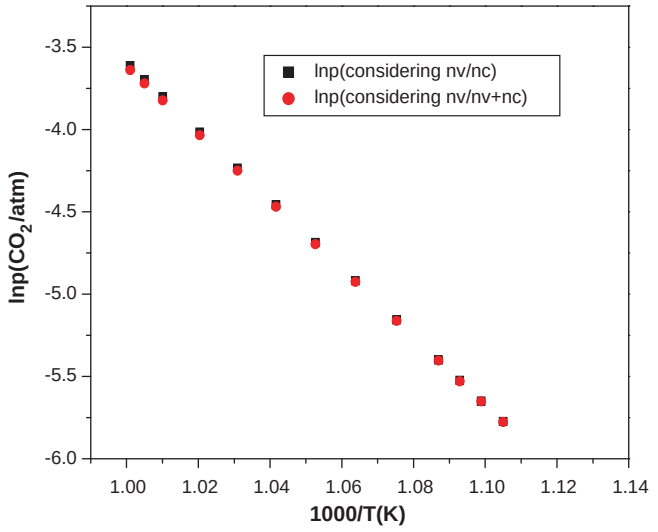

Fig. 8. The plot of $\ln p(CO_2(atm))$ as a function of $1/T$ (K) considering n_v and ignoring n_v in the denominator of Eq. (1) in the text.

The enthalpy changes for the decomposition of $CaCO_3$ at the mean temperature of 993 K using Eqs. (9) and (9a) were found to be 172.9 and 169.7 kJ/mol and using Eqs. (10) and (10a) were 172.9 and 171.1 kJ/mol, respectively.

The linear least squares fit Eqs. (9), (9a), (10) and (10a) derived from the DTG data can be compared with Eq. (11) reported by Vishwanathan et al. [18] derived from their latest conventional transpiration experiments presented below.

$$\ln\ p(CO_2(atm)) = \frac{-21355.72 \pm 666}{T} + 18.65 \pm 0.9 \qquad (11)$$

Similar equation derived from the best assessed literature data taken from ASTD compilation [17] can be expressed as

$$\ln\ p(CO_2(atm)) = \frac{-20388.38}{T} + 17.65 \qquad (12)$$

It is interesting to note that the enthalpy of thermal decomposition of $CaCO_3$ derived from the DTG measurements at the mean temperature of the experiment is very close to that reported by Vishwanathan et al. (177.6 kJ/mol) from their latest conventional isothermal measurements and also with that reported in the literature (171.1 kJ/mol) from the best assessed values of the dissociation pressure data available in the literature [17].

The credibility of the standard enthalpy value obtained by DTG method could be increased further by deriving the enthalpy of dissociation of $CaCO_3$ by observing the shift in the decomposition temperature of $CaCO_3$ with the increasing percentage of CO_2 in Ar–CO_2 mixture. The results obtained are listed in Table 4. The linear plot of $\ln p(CO_2(atm))$ versus $1/T$ derived from this data is presented in Fig. 7 and can be fitted to the equation of a line represented by Eq. (13)

$$\ln p(CO_2(atm)) = \frac{-19537.38 \pm 371.11}{T} + 16.85 \pm 0.38 \qquad (13)$$

The enthalpy for thermal decomposition derived from this plot was found to be 162.4 kJ/mol.

4.3. Determination of standard enthalpy of formation of $CaCO_3$ from the dissociation pressure data

The standard enthalpy of formation value for $CaCO_3$ was evaluated from the enthalpy change for the decomposition of $CaCO_3$ to CaO and CO_2 according to the following reaction

$$CaCO_3\ (s) = CaO\ (s) + CO_2\ (g) \qquad (14)$$

The standard enthalpy change for this reaction was evaluated at the mean temperature of the measurements from the temperature co-efficient of the evolved CO_2 pressure calculated either from the DTG curve or determined directly (Eq. (13)). The standard enthalpy of formation of $CaCO_3$ at this temperature (993 K) was obtained by using the data for the standard enthalpy of formation of CaO and CO_2 at 993 K from Ref. [17]. The standard enthalpy of formation of $CaCO_3$ at 298.15 K was derived using the value of standard enthalpy of formation of $CaCO_3$ at 993 K and the heat capacity data for $CaCO_3$,

Table 4
The dissociation pressure values of $CaCO_3$ derived from the ordinates of DTG curve at the flow rates of 2 and 4 ml/min compared with the values derived from equilibrium CO_2 pressure measurements and literature data.

Temperature (K)	$pCO_2 \times 10^3$/atm for 4 ml/min (considering (nv/nc)	$PCO_2 \times 10^3$/atm for 4 ml/min (considering $n_v/(n_v + n_c)$)	$PCO_2 \times 10^3$/atm for 2 ml/min (considering n_v/n_c)	$PCO_2 \times 10^3$/atm for 2 ml/min (considering $n_v/(n_v + n_c)$)	$PCO_2 \times 10^3$/atm (equilibrated under CO_2 atm)	$PCO_2 \times 10^3$/atm (literature)[a]
905	3.11	3.10	5.53	5.50	8.75	7.61
910	3.52	3.51	6.27	6.23	9.85	8.61
915	3.99	3.97	7.10	7.05	11.08	9.73
920	4.52	4.50	8.04	7.98	12.44	10.98
930	5.76	5.73	10.25	10.15	15.63	13.95
940	7.31	7.26	13.00	12.83	19.55	17.64
950	9.22	9.13	16.41	16.14	24.34	22.11
960	11.59	11.46	20.62	20.20	30.15	27.70
970	14.48	14.27	25.77	25.12	37.19	34.49
980	18.03	17.71	32.08	31.08	45.68	42.71
990	22.33	21.84	39.74	38.22	55.87	52.72
995	24.82	24.22	44.17	42.30	61.69	58.44
999	26.99	26.28	48.02	45.82	66.74	63.35

[a] Ref. [17].

CaO and CO_2 as a function of temperature available from Ref. [17]. The values of the standard enthalpy of formation of $CaCO_3$ derived by different methods at the mean temperature of these measurements are listed in Table 5. It is interesting to note that there is good agreement in the values of the standard enthalpy of formation of $CaCO_3$ obtained from the DTG curve, with those obtained by conventional transpiration technique [18], evaluated from the variation in the ambient CO_2 pressure with temperature (Eq. (13)) and that reported in the standard thermodynamic compilation [17].

5. Discussion

5.1. The conventional transpiration measurements

The main objective of the present investigation was to ascertain the possibility of using the derivative thermogravimetric (DTG) curve for acquisition of reliable thermodynamic data for the vaporization and thermal decomposition processes involving the evolution of the gaseous products. The conventional transpiration technique (see Section 2) can be suitably adopted to obtain such data. The first step in this procedure is to establish thermodynamic equilibrium between the vaporizing condensed phase and the vapor. The second step involves determination of the temperature coefficient of the vapor/dissociation pressure of the materials vaporizing under equilibrium condition from which the thermodynamic quantities such as the enthalpy of vaporization can be derived.

The thermodynamic equilibrium between the condensed phase and the vapor at the temperature of the experiment is established from the plateau region in the apparent pressure versus the flow rate plot. This plot generally consists of three regions [13]. In the initial slow flow rate region the apparent pressure decreases rapidly with the increasing flow rate. This region is followed by a plateau parallel to the flow rate axis and represents the equilibrium between the vapor and the condensed phase. The rate of vaporization in this region is much larger than the rate of vapor transport by the carrier gas, resulting in nearly constant vapor density around the sample thus facilitating the use of Dalton's law in the calculation of the partial pressure of the vapor in the mixture of the carrier gas and the vapor. The relative contribution to the total mass transport by diffusion caused by temperature gradient in this region of flow rate is much less compared to the amount of vapor transported by the carrier gas [13]. At very high flow rates there is rapid decrease of the apparent pressure with the increasing flow rate. The rate of vapor transport by the carrier gas is much faster than the rate of vaporization and hence this region represents the unsaturation of the carrier gas by the vapor and non-equilibrium condition. This region of the curve is therefore non-consquential and need not be obtained once the plateau region is established. In the present measurements the apparent pressure versus the flow rate plots are recorded only up to the plateau regions.

Figs. 3 and 6 clearly indicate that the thermodynamic equilibrium is indeed established between the vapor and the condensed phases in the isothermal transpiration experiments in these regions of the flow rate. After establishing the equilibrium condition, isothermal experiments are performed at several temperatures and the enthalpy of vaporization is derived from these data.

In the type of work reported in this investigation we need to establish the fact that at the heating rate employed for recording the DTG curve instantaneous equilibrium is established between the vapor and the condensed phases and there is minimal or no kinetic barrier for the vaporization process. The plateaus obtained in apparent pressure versus the flow rate in Figs. 3 and 6 confirm that in the region of the flow rates employed, in the present studies, the thermal equilibrium between the vapor and the condense

Table 5
The standard enthalpy of formation of $CaCO_3$ at 298.15 K calculated from the slope of the $\ln p(CO_2(atm))$ versus $1/T$ (K) data obtained from DTG experiments carried out at different flow rates, compared to the values reported by other investigators.

Experimental conditions	ΔH (decomposition) at 993 K kJ/mol	Enthalpy of formation of $CaCO_3$ at 993 K kJ/mol	Standard enthalpy of formation of $CaCO_3$ at 298.15 K kJ/mol
2 ml/mivnn (DTG)	172.9 (ignoring n_v)	−1201.6	−1210.0[a]
2 ml/min (DTG)	169.7 (including n_v)	−1198.4	−1206.8[a]
4 ml/min (DTG)	172.9 (ignoring n_v)	−1201.6	−1210.0[a]
4 ml/min (DTG)	171.1 (including n_v)	−1199.8	−1208.2[a]
Variation of ambient CO_2 pressure (flow rate of Ar–CO_2 8 ml/min)	162.4	−1191.1	−1199.5[a]
Conventional transpiration method	177.6	−1206.3	−1214.7 Ref. [18]
Lit. data	171.1	−1200.9	−1209.3 Ref. [17]

[a] Present work.

phase/s exists at the temperatures of the experiments. Generally, the plateau region is established at the intermediate temperature of the temperature range over which the vapor pressure is measured. It is important to note that the region of flow rate in which the plateau is observed depends on the system investigated and the kinetics of the process involved. This is obvious from the plateaus observed in the case of vaporization of CdI_2 and thermal decomposition of $CaCO_3$. In the latter case the plateau is observed in the region of much slower flow rate.

The plateau regions obtained in the present experiments involved heating of the sample at 1 K/min and holding the temperature constant at the intermediate temperature of the measurements. These temperatures were 757 and 993 K, respectively for CdI_2 and $CaCO_3$. Isothermal mass loss was then monitored at these temperatures for different flow rates of the carrier gas. The plateaus obtained (Figs. 3 and 6) at these temperatures show that the equilibrium between the vapor and condensed phase is established in these flow rate regions.

The good agreement in the vapor/dissociation pressure data and the enthalpy of vaporization obtained in the present work derived from the DTG curve with that obtained by conventional isothermal transpiration experiments in the case of CdI_2 and $CaCO_3$ establishes the fact that in the vaporization and thermal dissociation processes studied in the present work thermal equilibrium between the condensed phase and the vapor is established much faster and the thermodynamic data obtained in the shortest possible time is sufficiently accurate and comparable with that obtained by other conventional methods. The thermodynamic data obtained for the vaporization of CdI_2 and thermal decomposition of $CaCO_3$ further indicates that the new procedure of application of DTG for the evaluation of thermodynamic data is valid for the congruent vaporization of solids or liquids as well as heterogeneous non-congruent vaporization of the condensed phases.

Good agreement of the vapor and dissociation pressures and enthalpy changes derived from DTG with those obtained by other standard techniques (Tables 2, 4 and 5) indicates that nearly instantaneous equilibrium between the condensed phases and the vapor is established during the DTG experiment and reliable thermodynamic data can be obtained from such curves recorded under optimum heating rate and the sweep rate of the carrier gas passed over the sample.

6. Conclusion

The vapor pressure and dissociation pressure of materials can be evaluated and the enthalpy of vaporization/dissociation derived from a single DTG curve recorded for the process at the slowest possible heating rate and the optimum sweep rate of the carrier gas. This method enables determination of the relevant thermodynamic quantities such as the standard enthalpy and the Gibbs energy change for the reaction and hence the standard enthalpy of formation of the materials, in the shortest possible time compared to that obtained by conventional vapor pressure measurements since it involves a single DTG experiment followed by the determination of the plateau region for the confirmation of establishment of the thermodynamic equilibrium condition between the vapor and the condensed phase. To our knowledge, this is the first time the use of DTG is proposed for acquisition of such thermodynamic data.

References

[1] R. Mishra, S.R. Bharadwaj, A.S. Kerkar, S.R. Dharwadkar, J. Nucl. Mater. 240 (1997) 236–240.
[2] S.R. Bharadwaj, R. Mishra, M. Ali (Basu), A.S. Kerkar, S.R. Dharwadkar, J. Nucl. Mater. 275 (1999) 201–205.
[3] M. Ali (Basu), R. Mishra, S.R. Bharadwaj, A.S. Kerkar, S.R. Dharwadkar, D. Das, J. Nucl. Mater. 299 (2001) 165–170.
[4] R. Mishra, M. Ali (Basu), S.R. Bharadwaj, A.S. Kerkar, D. Das, S.R. Dharwadkar, J. Alloy Compd. 290 (1999) 97–102.
[5] K. Hilpert, M. Miller, H. Gerads, H. Nickel, Ber. Bunsenges. Phys. Chem. 94 (1990) 40–47.
[6] K. Hilpert, D. Kobertz, V. Venugopal, M. Miller, H. Gerad, F.J. Bremmer, H. Nickel, Z. Naturfosch. 42 a (1987) 1327–1332.
[7] C.B. Alcock, G.W. Hooper, Proc. Royal Soc. A 254 (1960) 551–561.
[8] O. Kubaschewski, C.B. Alcock, P.J. Spencer, Materials Thermochemistry, sixth ed., Pergamon Press, Oxford, 1993.
[9] J.W. Hastie (Ed.), Characterization of High Temperature Vapors and Gases, vol. 1, 1978, Special NBS Publication No. 561.
[10] J.L. Margrave (Ed.), Characterization of High Temperature Vapors, John Wiley and Sons Inc., 1967.
[11] R.V. Regnault, Ann. Chim. 15 (1845) 129.
[12] P.W. Atkins, Text Book of Physical Chemistry, Oxford University Press, 1998.
[13] U. Merten, W.E. Bell, in: J.L. Margrave (Ed.), Characterization of High Temperature Vapors, John Wiley and Sons Inc., 1967, pp. 91–114.
[14] H. Kvande, P. Wahlbeck, Acta Chem. Scand. A 30 (1976) 297–302.
[15] S.R. Dharwadkar, A.S. Kerkar, M.S. Samant, Thermochim. Acta 217 (1993) 175–186.
[16] K. Skudlarski, J. Dudek, J. Kapala, J. Chem. Thermodyn. 19 (1987) 857–862.
[17] ASTD, Computer Aided Reference book in Thermodynamical, Thermochemical and Thermophysical properties of Species, Version 2.0 by Below G. V., Trusov B.G., Moscow, ©1983–1995.
[18] R. Viswanathan, T.S. Lakshmi Narasimhan, S. Nalini, Thermal analysis, in: P.C. Kalsi, R.V. Pai, M.R. Pai, S.R. Bharadwaj, V. Venugopal (Eds.), Proc. 17th Natl. Symp. on Thermal Analysis, Kurukshetra University, March 9–11, 2010, pp. 168–170.
[19] J.O. Hill, For Better Thermal Analysis, third ed., ICTA, London, 1991.